Journal of Applied Mechanics and Technical Physics, Vol. 44, No. 5, pp. 640–647, 2003

EXPERIMENTAL STUDY OF SUPERSONIC FLOW AROUND TRUNCATED CONES AT INCIDENCE

M. D. Brodetsky and A. M. Shevchenko

UDC 519.6+533.6.07

Results of an experimental study of supersonic flow around truncated cones with cone half-angles of 20, 30, *and* 40°, *performed at Mach numbers* $M = 2$, 3, and 4 *within the range of angles of attack up to* 20°, *are presented. A relationship is established between the emergence of an internal shock wave and the character of pressure distribution along the generatrix of the truncated cone. It is shown that the known boundaries of regimes obtained for axisymmetric flow around sharp and blunt cones can be used to predict flow regimes in the vertical plane of symmetry of the truncated cone at incidence.*

Key words: *truncated cone, supersonic flow regimes, shock wave.*

Introduction. The necessity of experimental investigations of supersonic flow around truncated cones is caused by the following basic reasons. First, the orifice of one of the most widespread pneumometric probes for simultaneous determination of the direction, Mach number, and total pressure in a three-dimensional flow is shaped as a truncated cone (see, e.g., [1]). Therefore, detailed data on the pressure distribution and flow structure near the surface of this class of bodies is necessary to solve methodical problems related to the choice of the orifice geometry, to construct the mathematical model of the probe, and to identify anomalous regimes of probe operation. Second, the truncated cone is a particular case of blunted forebodies used in aerospace engineering. Based on numerical calculations, it was shown [2] that the use of a flat face or a strongly oblate ellipsoid instead of conventional spherical bluntness as a forebody of reentry vehicles leads to an increase in static stability, greater resistance to erosion, etc. Third, the truncated cone is one of the classical aerodynamic shapes; the flow around it is accompanied by the formation of a curved shock wave, local subsonic and supersonic regions, and internal shock waves. Thus, experimental data on the flow in the vicinity of the truncated cone is a good test for verification of numerical methods developed for complicated supersonic spatial flows.

Bodies with a finite bluntness radius were mainly considered in numerous papers (see, e.g., [3] and the references cited there). Some studies were performed for axisymmetric flows around blunted bodies in the form of a flat face on a cylinder or a cone [4, 5].

The objective of the present work is to study supersonic flow around truncated cones at incidence. The analysis of the results obtained allows identification of previously unknown features of the flow and conditions for changes in the flow regime.

1. Models and Experimental Technique. The supersonic flow around truncated cones with a dead-end central orifice was considered on a set of models whose layout is schematically shown in Fig. 1. The model was a cylindrical body with a replaceable forebody shaped as a truncated cone. The cylinder diameter was $D = 30$ mm, the cone half-angle was $\omega = 20$, 30, and 40°, and the diameter of the small base of the cone was $d = D/3$. Sixteen orifices 0.5 mm in diameter for static pressure measurements were located in two mutually perpendicular planes on the side surface of the cone (four orifices on one generatrix with a step equal to 20% of its length). The dimensionless distance s/d was varied (s is the distance counted along the generatrix from the end face) (Fig. 1). The end face of the model had a dead-end central orifice of diameter $0.5d$ and depth $2.2d$. A pneumometric pipeline for measuring stagnation pressure at the end face was connected to the bottom of this orifice. To reduce sensitivity to variation of the angle of attack, the central orifice was counterbored at an angle of 90°.

Institute of Theoretical and Applied Mechanics, Siberian Division, Russian Academy of Sciences, Novosibirsk 630090. Translated from Prikladnaya Mekhanika i Tekhnicheskaya Fizika, Vol. 44, No. 5, pp. 45–54, September–October, 2003. Original article submitted October 2, 2001; revision submitted January 21, 2003.

 0021-8944/03/4405-0640 $25.00

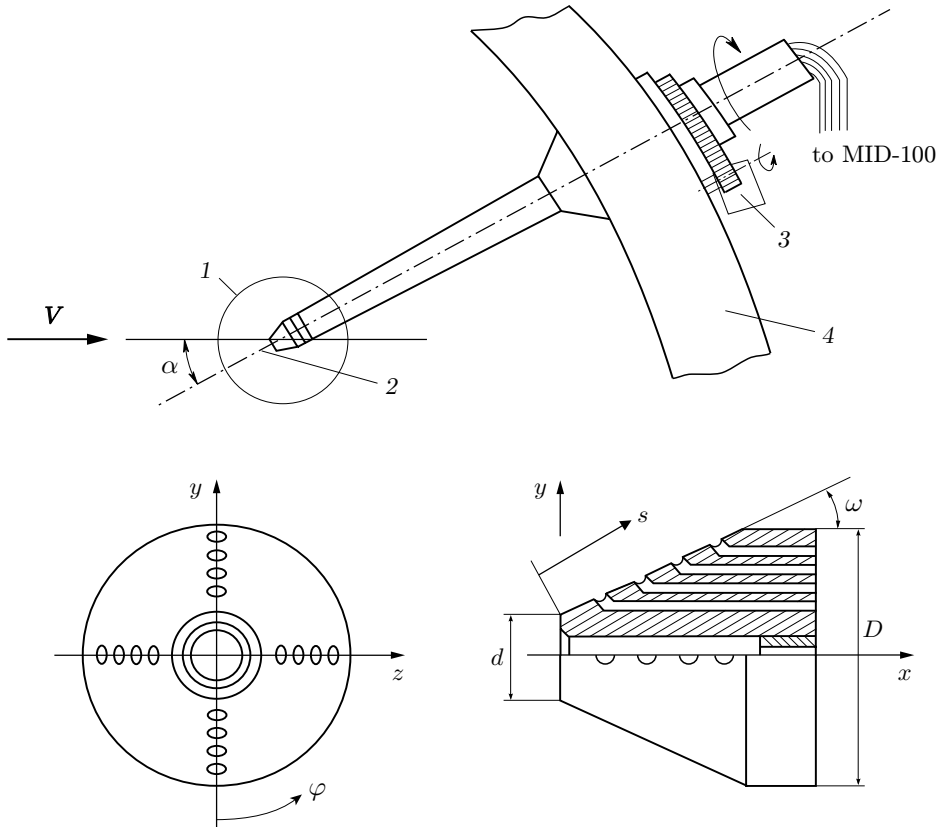

Fig. 1. Model and schematic of its mounting in the wind-tunnel test section: 1) replaceable forebody; 2) axis of the AB-313M balance; 3) mechanism for changing the rolling angle of the model; 4) scimitar suspension of the AB-313M aerodynamic balance.

The experiments were performed in a T-313 supersonic wind tunnel of the Institute of Theoretical and Applied Mechanics of the Siberian Division of the Russian Academy of Sciences for Mach numbers M = 2.03, 3.02, and 4.03 and the corresponding Reynolds numbers $\mathrm{Re}_1 = 23.5 \cdot 10^6$, $30 \cdot 10^6$, and $48 \cdot 10^6$ m^{-1}. The total pressure in the plenum chamber of the T-313 wind tunnel was $P_0 = 2.0$, 4.3, and 10.4 kg/cm^2, respectively. The stagnation pressure behind the normal shock ahead of the model forebody remained almost unchanged and reached $P_0' \approx 1.4$ kg/cm^2 for all regimes.

The experiments included flow visualization in the vertical plane of symmetry of the model (schlieren pictures were obtained by an IAB-451 shadowgraph), visualization of the limiting streamlines on the side surface of the truncated cone (by the oil-film technique), and pressure measurement on the model surface (by an MID-100 multichannel pressure meter with accuracy of 0.3% [6]). In addition, for the cone with $\omega = 30°$ and M = 2.03, 2.28, 2.52, 3.02, and 4.03, the static pressure on the side surface of the model was measured in cross sections $s/d = 1/3$, 2/3, 1, and 4/3.

In the experiment, the model was mounted in the scimitar suspension of the AB-313M mechanical balance whose α-mechanism provided variation of the angle of attack α. For pressure measurements, the model was mounted into a special device with an electromechanical drive providing the possibility of model rotation around its longitudinal axis. The data on pressure distribution over the model surface were obtained with a step of 15° along the coordinate φ (Fig. 1).

2. Test Results. Figure 2 shows a typical Schlieren picture of the flow around a truncated cone for M = 4, $\omega = 20°$, and $\alpha = 10°$. The photographs obtained with two different positions of the sheet of the IAB-451 shadowgraph show a detached bow shock wave, a separation region near the end face, and an internal shock wave. Any noticeable oscillations of the bow shock could not be identified by visual observation or by comparing photographs taken at different times under identical test conditions. Nevertheless, we cannot exclude its high-frequency oscillations, though no special studies were performed. The reason for flow separation and formation of the internal shock is flow overexpansion in the Prandtl–Mayer flow near the corner point [5, 7, 8] and its subsequent

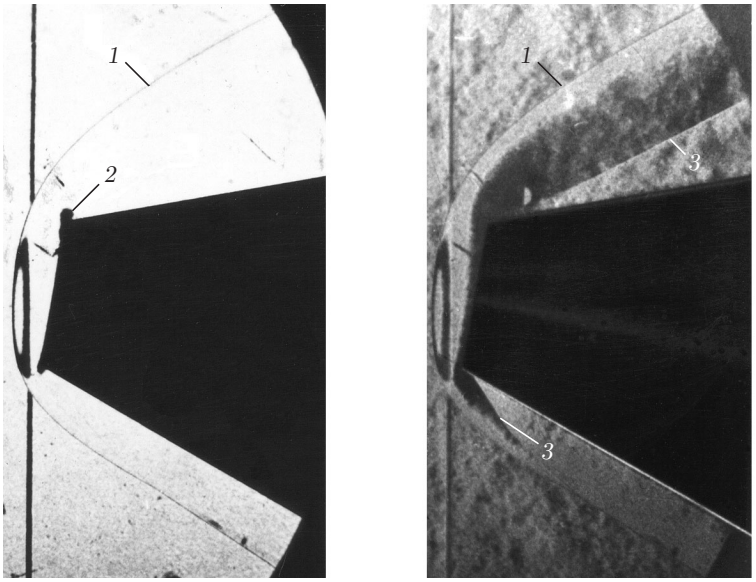

Fig. 2. Schlieren pictures of the flow ($\omega = 20°$, M = 4, and $\alpha = 10°$): 1) bow shock wave; 2) flow-separation region; 3) internal shock wave.

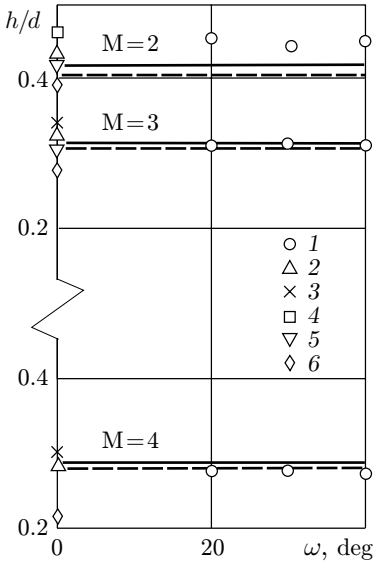

Fig. 3. Distance between the bow shock wave and the end face: 1) data of the present work; 2) data of [4]; 3) data of [7]; 4) data of [9]; 5) data of [5]; 6) data of [8]; the solid and dashed curves refer to calculations by the empirical formulas of [11] and [12], respectively.

compression to a pressure equal, in an isentropic flow at a large distance from the end face, to the static pressure on the surface of an equivalent sharp cone (with the same half-angle ω). Internal shock waves were found both in experimental studies [4, 5, 8, 9] and in inviscid computations [3, 7, 10] but only for bodies with a discontinuity of the generatrix curvature. The discontinuity of the generatrix curvature was not always accompanied by the formation of an internal shock wave [3, 8, 10].

One important characteristic of the flow is the distance h between the bow shock wave and the end face (stand-off distance). Figure 3 shows the dependence of h/d on the cone half-angle ω in an axisymmetric flow around a truncated cone ($\alpha = 0$). The same figure shows the results of experimental [4, 5, 8, 9] and numerical [7] works for a cylinder with a flat end ($\omega = 0$). The solid curves were obtained with the use of the empirical relation [11], which has the form $h/d = [2.8 \tan \omega_{\rm cr}(\mathrm{M}_\infty)]^{-1}$ for the truncated cone and is valid for $\omega \leqslant \omega_{\rm cr}$ and $\mathrm{M} \geqslant 2$. Here $\omega_{\rm cr}(\mathrm{M}_\infty)$ is the maximum half-angle of the sharp cone for which the flow with an attached shock wave is still possible. The dashed

curves show the calculations results for $h/d = \text{const}$ by the empirical formula $h/d = 0.23\sqrt{(\mathrm{M}^2+5)/(\mathrm{M}^2-1)}$ [12]. With allowance for the scatter of data obtained in various works, the results of the present work confirm the conclusion that the stand-off distance of the bow shock with a fixed Mach number is determined by the bluntness shape only and is independent of the cone half-angle for $\omega \leqslant \omega_{\mathrm{cr}}(\mathrm{M}_\infty)$. With increasing Mach number, as it follows from Fig. 3 and above-given empirical relations, the bow shock wave approaches the cone surface. The effect of the Mach number on the value of h/d becomes weaker. It was shown in [3, 7] that, in the flow around bodies with a sonic inflection (the sonic line arrives at the corner point), the supersonic flow region near the body surface has a small section that affects the flow in the subsonic region (in this case, for $\mathrm{M} \leqslant 1.2$, the minimum influence region of type II in the classification of [7] is observed). Therefore, the value of h/d can be expected to depend on the angle ω. Within the experimental error, however, the influence of the angle ω on h/d was not observed.

For $\omega \geqslant \omega_{\mathrm{cr}}(\mathrm{M}_\infty)$, the stand-off distance of the bow shock is determined by the cone half-angle and does not depend on the bluntness shape, i.e., the distance is the same as on an equivalent sharp cone. In this regime, as is shown in [13, 14], the distance from the apex of the equivalent sharp cone and the shock wave, normalized to the diameter of the larger base of the cone, depends on the angle ω almost linearly.

Figure 4 shows the results of processing the Schlieren pictures of the flow in the vertical plane of symmetry of the truncated cone, which give an idea of the shape and position of the bow and internal shock waves. Before the interaction of the internal and bow shock waves, the position of the bow shock largely depends on the angle of attack: with increasing α, it approaches the cone surface on the windward side of the model and, vice versa, goes away on the leeward side (in this case, it is more correct to speak about the half-planes $\varphi = 0$ and 180°, respectively). The distance between the end face and the bow shock, measured along the longitudinal axis of the model, is almost independent of the angle of attack.

Interaction of the internal shock wave with the bow shock wave increases the slope of the latter. After interaction, the position of the bow shock with respect to the cone surface depends weakly on the angle of attack, especially for cones with $\omega = 30$ and 40°.

The position of the internal shock wave with respect to the end face of the model depends on the angle of attack and on the cone angle. With increasing α, the internal shock approaches the edge on the windward side and departs from the edge on the leeward side. With increasing ω, this dependence becomes weaker, and the internal shock wave is formed closer to the edge. The maximum distance from the end face of the model is observed for $\alpha = 20^\circ$ and does not exceed $0.3d/\sin\omega$ in all cases considered, which is 30% of the length of the truncated cone generatrix for cones with the ratio of diameters $D/d = 3$.

Figure 5 shows a typical pressure distribution along the circumferential coordinate φ. The experimental pressure distribution is in qualitative agreement with a similar dependence $P/P_0'(\varphi)$ obtained in calculating the inviscid flow around a sharp cone [15]. As for the sharp cone, the dependence $P/P_0'(\varphi)$ at high angles of attack has a minimum in the interval $90^\circ < \varphi < 180^\circ$. The regression analysis of the dependences $P/P_0'(\varphi)$ performed for the entire range of examined parameters shows that the pressure distribution over the circumferential coordinate φ is adequately (by the F criterion [16]) described by the first three terms of expansion into the Fourier series in cosines with expansion coefficients depending on the Mach number and angle of attack. An exception was the results of data processing for the cross section $s/d = 0.6$ for $\omega = 40^\circ$ and $\alpha = 20^\circ$ whose adequate representation as a Fourier series requires the third and fourth harmonics. The results obtained form the basis for the mathematical model of the multichannel conical pneumometric probe for simultaneous measurements of the velocity-vector direction, Mach number, and total pressure in a three-dimensional flow with direct determination of one of the measured parameters [17].

Figure 6 shows the pressure distribution along the generatrix of the truncated cone in the half-planes $\varphi = 0$ and 180°. The same figure shows the calculation results for an inviscid flow around a sharp cone, which are in good agreement with the experimental results (as $x \to \infty$, the pressure on the surface of a blunted cone is known to tend to a value equal to the static pressure on the equivalent sharp cone [3, 11]).

A comparison of flow visualization and pressure measurements revealed the following feature. If the internal shock wave exists, the pressure behind the separation region does not decrease with distance from the end face. Vice versa, if there is no internal shock wave, the pressure decreases with distance from the end face.

Figure 7 shows the boundaries of regimes of axisymmetric flows around sharp and blunted cones, which were calculated in [3, 18]. Curve I refers to the boundary between the flow regimes around the sharp cone with a detached shock wave (above curve I) and attached shock wave (below curve I). Curve II is the boundary of

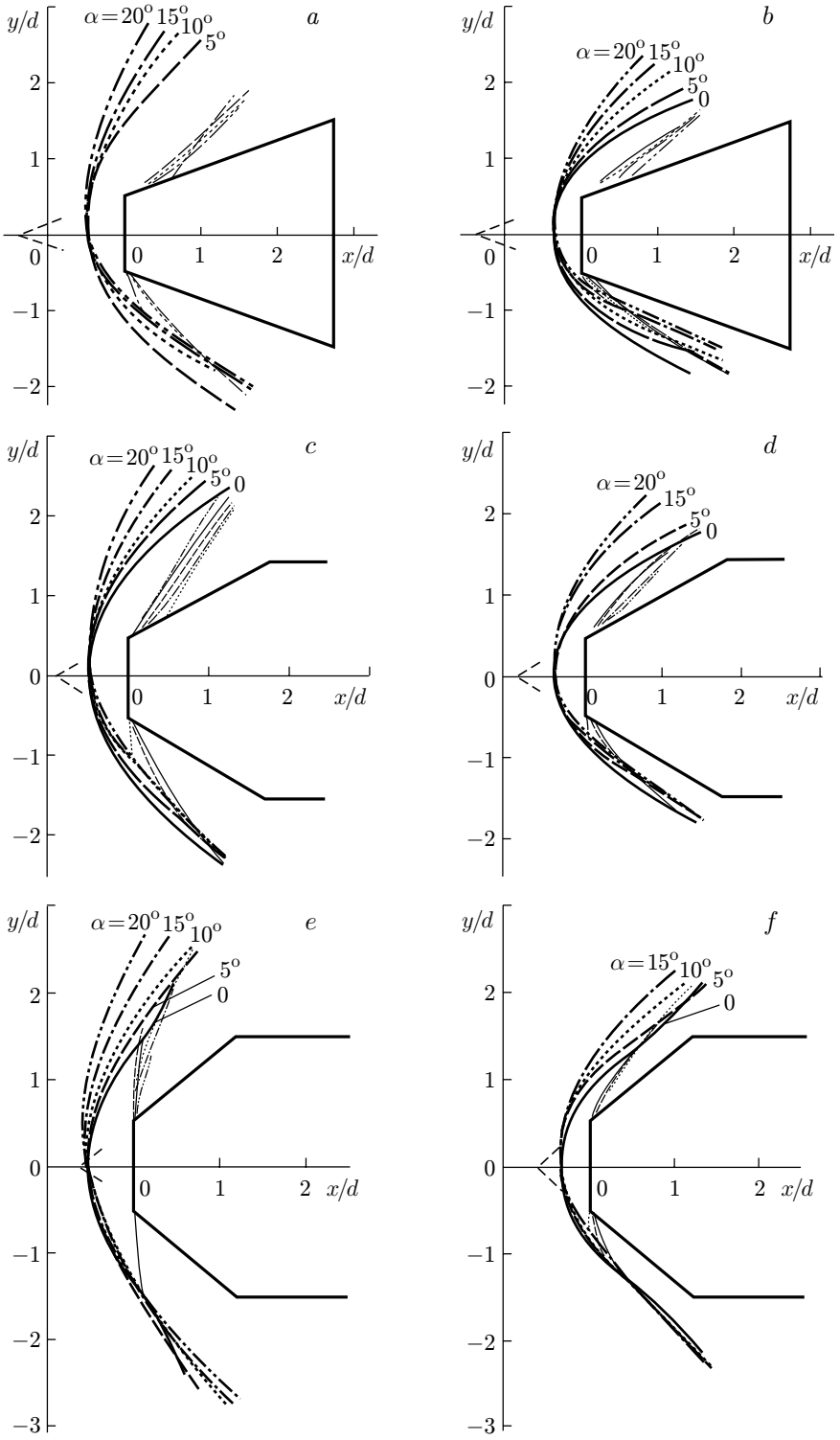

Fig. 4. Position of the bow shock (bold curves) and internal shock waves (thin curves) for M = 2 and $\omega = 20°$ (a), M = 4 and $\omega = 20°$ (b), M = 2 and $\omega = 30°$ (c), M = 4 and $\omega = 30°$ (d), M = 2 and $\omega = 40°$ (e), and M = 4 and $\omega = 40°$ (f).

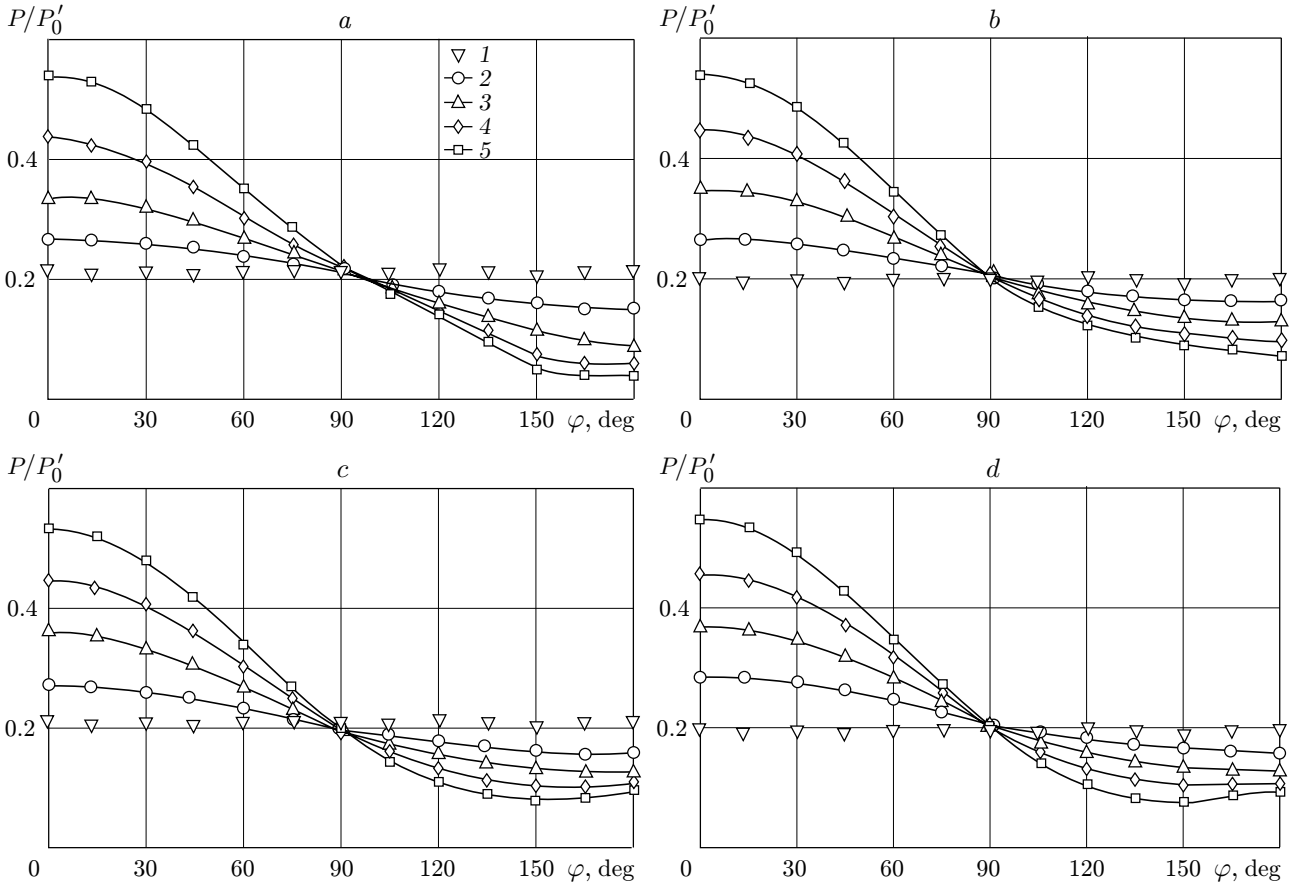

Fig. 5. Pressure distribution along the circumferential coordinate ($\omega = 20^\circ$ and M = 3) for $s/d = 0.6$ (a), 1.2 (b), 1.8 (c), and 2.4 (d): $\alpha = 0$ (1), 5 (2), 10 (3), 15 (4), and 20° (5).

flow regimes around the blunted cone. For $\omega > \omega_*$ and $x \to \infty$, we have M < 1 near the body surface, i.e., the subsonic region is unbounded. For $\omega < \omega_*(\mathrm{M}_\infty)$, the flow is completely supersonic at a sufficient distance from the forebody of the blunted cone, and the subsonic region is bounded [3, 19]. The points is Fig. 7 show various regimes investigated in the present work and in [4]. The circles and triangles correspond to an axisymmetric flow ($\alpha = 0$). The squares show the fictitious values ω_f in the case of the flow around the truncated cone at incidence, which were assumed to be $\omega_\mathrm{f} = \omega + \alpha$ for $\varphi = 0$ and $\omega_\mathrm{f} = \omega - \alpha$ for $\varphi = 180^\circ$. The open points refer to flow regimes in which the internal shock wave was registered and the pressure did not decrease with distance from the end face. The filled points correspond to flow regimes around the truncated cone without formation of the internal shock wave and with a decrease in pressure with distance from the end face. The points located below curve II correspond to the case with $P/P_0' > 0.528$ in the cross section remote from the end face, i.e., the local Mach number near the surface is lower than unity (indeed, because of the internal shock waves, the local total pressure can be only lower than P_0'; therefore, the following relation is valid for the local Mach number: $\mathrm{M} \leqslant \sqrt{5[(P_0'/P)^{2/7} - 1]}$).

It is seen from Fig. 7 that the filled points are located above curve I and the open points are located below this curve. Hence, the known boundary of axisymmetric flow regimes around the sharp cone $\omega_\mathrm{cr}(\mathrm{M}_\infty)$ can be used to predict the features of the flow around the truncated cone at incidence: if $\omega_\mathrm{f} > \omega_\mathrm{cr}(\mathrm{M}_\infty)$, the pressure on the side surface of the truncated cone decreases with distance from the end face and there are no internal shock waves. If $\omega_\mathrm{f} < \omega_\mathrm{cr}(\mathrm{M}_\infty)$, the flow around the truncated cone is accompanied by the formation of the internal shock wave and by an increase in pressure with distance from the end face.

It is also seen in Fig. 7 that the points corresponding to flow regimes with an unbounded subsonic region lie above curve II and the points corresponding to regimes with a bounded subsonic region lie below curve II. Hence, this boundary can also be used to predict the features of the flow around the truncated cone at incidence: if $\omega_\mathrm{f} > \omega_*(\mathrm{M}_\infty)$, we have M < 1 far from the end face, i.e., the subsonic region is unbounded. If $\omega_\mathrm{f} < \omega_*(\mathrm{M}_\infty)$, we have M > 1 far from the end face, i.e., the subsonic region is bounded.

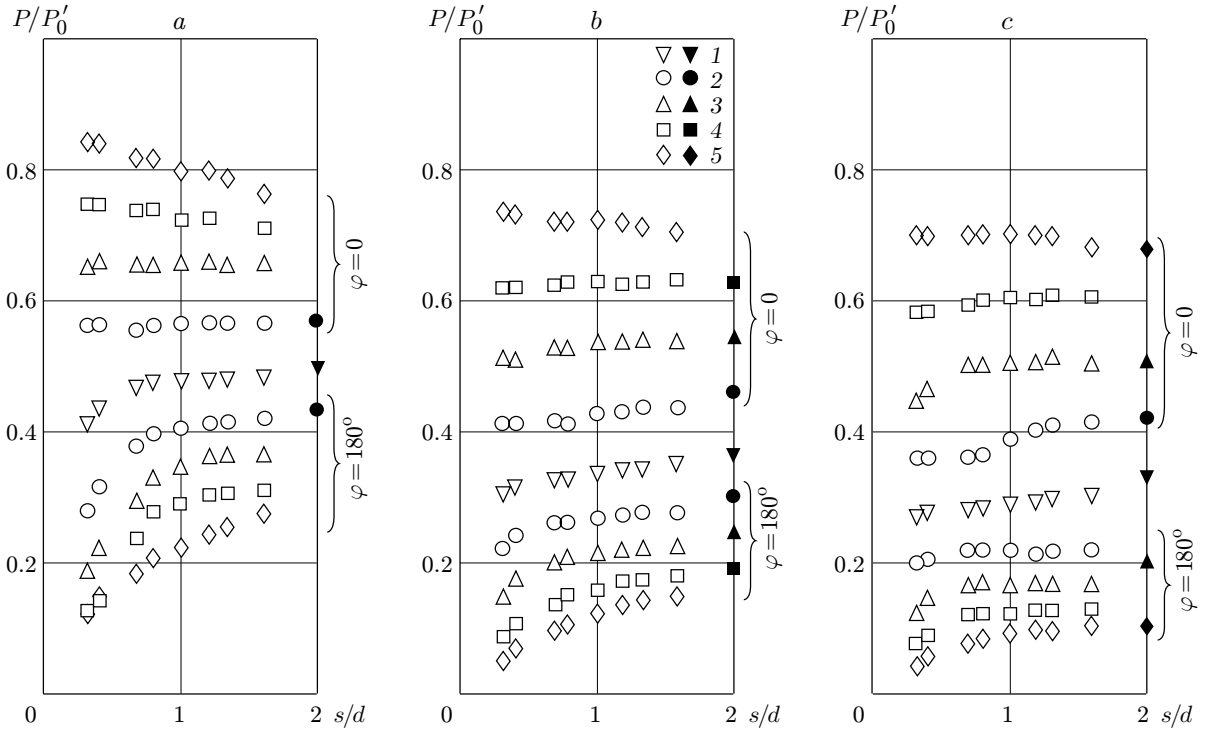

Fig. 6. Pressure distribution along the generatrix in the vertical plane of symmetry ($\omega = 30°$) for M = 2 (a), 3 (b), and 4 (c); the open points show the data of the present work and the filled points refer to the data for the sharp cone [15]; $\alpha = 0$ (1); 5 (2), 10 (3), 15 (4), and 20° (5).

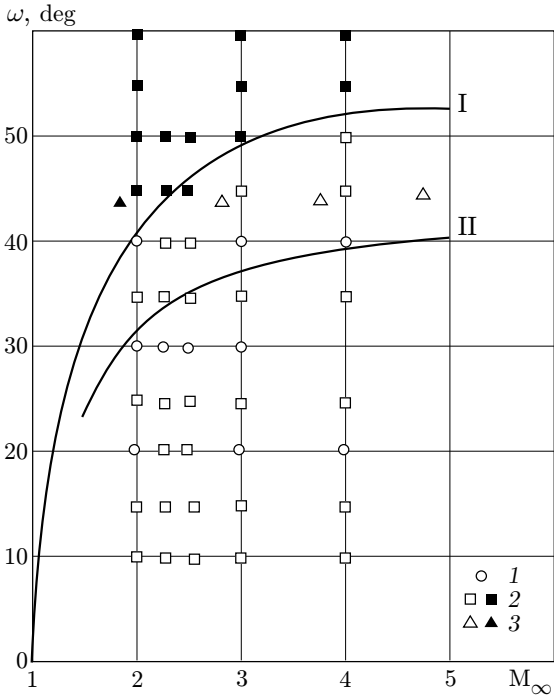

Fig. 7. Flow chart for blunted cones: ω_{cr} (I) and ω_* (II); curves 1 and 2 show the data of the present work [ω for $\alpha = 0$ (1) and ω_f (2)] and curve 3 shows the data of [4] (ω for $\alpha = 0$).

It should be noted that the condition $P/P_0' < 0.528$ holds for $\omega_* < \omega_f < \omega_{cr}$ at a comparatively small distance from the end face. Hence, the flow near the surface is supersonic, which is confirmed by origination of internal shock waves in these regimes. In remote cross sections, we have $P/P_0' > 0.528$, i.e., the flow is subsonic. Therefore, the use of boundary II is correct at large distances from the end face only, which follows from the conditions of obtaining this boundary [19].

Conclusions. A supersonic flow around truncated cones with half-angles $\omega = 20$, 30, and 40° was considered in the range of Mach numbers $M = 2$–4 and angles of attack up to 20°.

Detailed data on the position of the bow and internal shock waves were obtained, and the pressure distribution on the side surface of the cone was measured.

It was found that origination of the internal shock wave determines the character of pressure distribution along the generatrix of the truncated cone. If the internal shock wave appears (does not appear), the pressure with distance from the end face tends to an asymptotic value (pressure on the equivalent sharp cone) from below (above).

It was shown that the known boundaries of flow regimes $\omega_{cr}(M_\infty)$ and $\omega_*(M_\infty)$ obtained for an axisymmetric flow around sharp and blunted cones can be used to predict flow regimes in the vertical plane of symmetry of the truncated cone at incidence.

REFERENCES

1. A. N. Petunin, *Methods and Technique for Measuring Gas-Flow Parameters* [in Russian], Mashinostroenie, Moscow (1996).
2. T. C. Lin, W. R. Grabowski, and K. E. Yelmgren, "The search for optimum configurations for re-entry vehicles," *J. Spacecraft Rockets*, **21**, No. 2, 142–149 (1984).
3. A. N. Lyubimov and V. V. Rusanov, *Gas Flow Around Blunt Bodies* [in Russian], Nauka, Moscow (1970).
4. *Handbook of Supersonic Aerodynamics. Body of Revolution*, Vol. 3, Sec. 8, Washington (1961).
5. G. M. Ryabinkov and A. G. Ryabinkov, "Experimental study of the flow around a cylinder with a flat end face," in: *Problems of Applied Mathematics and Mechanics* [in Russian], Nauka, Moscow (1971), pp. 269–277.
6. M. A. Amelina, M. D. Brodetsky, I. I. Volonikhin, et al., "MID-100 multichannel pressure meter," in: *Methods and Techniques of Aerophysical Research* [in Russian], Inst. Theor. Appl. Mech., Sib. Div., Acad. of Sci. of the USSR, Novosibirsk (1978), pp. 98–113.
7. O. M. Belotserkovskii and Yu. M. Davydov, *Method of Coarse Particles in Gas Dynamics* [in Russian], Nauka, Moscow (1982).
8. D. R. Philpott, "An investigation into the flow around a family of elliptically nosed cylinders at zero incidence at M = 2.5 and 4.0," *Aeronaut. Quart.*, **23**, Part 4, 315–326 (1972).
9. M. Van Dyke (assemb.), *An Album of Fluid Motion*, Parabolic Press, Stanford, California (1982).
10. A. N. Lyubimov, "Existence of internal shock waves in the gas flow around blunted cones," *Dokl. Akad. Nauk SSSR*, **191**, No. 4, 783–786 (1970).
11. Yu. D. Shevelev, *Spatial Problems of Computational Aerohydrodynamics* [in Russian], Nauka, Moscow (1986).
12. N. F. Krasnov, V. I. Koshevoi, A. N. Danilov, and V. F. Zakharchenko, *Rocket Aerodynamics* [in Russian], Vysshaya Shkola, Moscow (1968).
13. L. C. Ward and P. G. Pugh, "Shock standoff distances of blunt and sharp cones," *AIAA J.*, **6**, No. 10, 2018–2019 (1968).
14. I. I. Amarantova, V. G. Bukovshin, and V. I. Shustov, "Flow around cones with large half-angles," *Uch. Zap. TsAGI*, **18**, No. 2, 110–113 (1987).
15. K. I. Babenko, G. P. Voskresenskii, A. N. Lyubimov, and V. V. Rusanov, *Spatial Ideal-Gas Flow Around Smooth Bodies* [in Russian], Nauka, Moscow (1964).
16. D. Himmelblau, *Process Analysis by Statistical Methods*, McGraw Hill, New York (1970).
17. M. D. Brodetsky, G. P. Ol'khovikov, A. M. Kharitonov, et al., "Technique for measuring the direction and Mach number of a three-dimensional supersonic flow," *Uch. Zap. TsAGI*, **15**, No. 3, 136–139 (1984).
18. N. F. Krasnov, *Aerodynamics of Bodies of Revolution* [in Russian], Oborongiz, Moscow (1958).
19. Yu. D. Terent'ev, "Shape of the sonic line in a supersonic perfect-gas flow around a blunted wedge," *Dokl. Akad. Nauk SSSR*, **247**, No. 2, 319–323 (1979).